Brain Struct Funct (2007) 212:245–253
DOI 10.1007/s00429-007-0157-x

ORIGINAL ARTICLE

A proposal for MRI-based parcellation of the frontal pole

John P. John · B. S. Yashavantha · Mokthar Gado · R. Veena · Sanjeev Jain · S. Ravishankar · John G. Csernansky

Received: 24 March 2007 / Accepted: 24 August 2007 / Published online: 11 October 2007

Abstract The frontal pole (FP), which largely overlaps with Brodmann's area (BA) 10, is the rostral-most part of the hominid cerebral cortex, and plays a critical role in complex aspects of human cognition. The existing conventions suggested for MRI-based parcellation of this important frontal subdivision have limited cytoarchitectonic meaning with regard to the demarcation of the FP from adjacent prefrontal subdivisions. In this paper, we propose the coronal section containing the anterior termination of the olfactory sulcus (ATOS) as an easy-to-identify landmark for FP parcellation that largely overlaps with the cytoarchitectonic distinction between BA 10 and the more posterior cytoarchitectonic subdivisions of the PFC. Manual segmentation-based parcellation of the FP using the proposed landmark in 20 healthy volunteers yielded highly reliable (standardized item alpha = 0.92) volumetric estimates [right FP volume = 8.421 cm^3 (SE = 0.773, range 3.107–15.741); left FP volume = 8.039 cm^3 (SE = 0.708, range 2.234–12.956)]. The volumetric measurements of right FP generated in the present study were comparable to those reported in a prior study of BA 10 using histological sections and stereological techniques (Semendeferi et al. In: Am J Phys Anthropol 114:224–241, 2001). Therefore, in the absence of a naturally occurring sulcal boundary, the proposed method for parcellation of the FP can provide unbiased volume estimations for studies of healthy and disordered populations of subjects.

Keywords Frontal pole · Parcellation · MRI · Olfactory sulcus · Landmark

J. P. John (✉) · B. S. Yashavantha · R. Veena · S. Jain
Department of Psychiatry, National Institute of Mental Health and Neurosciences (NIMHANS), P.B. No. 2900, Dharmaram P.O., Hosur Road, Bangalore, Karnataka 560029, India
e-mail: jpj@nimhans.kar.nic.in; jpjinc@yahoo.com

S. Ravishankar
Department of Neuroimaging and Interventional Radiology (NIIR), National Institute of Mental Health and Neurosciences (NIMHANS), Bangalore, India

J. G. Csernansky
Department of Psychiatry, Washington University School of Medicine, St Louis, MO, USA

M. Gado
Department of Radiology, Washington University School of Medicine, St Louis, MO, USA

Introduction

The frontal pole (FP), also referred to as "anterior prefrontal cortex", "fronto-polar cortex" or "rostral prefrontal cortex" is the anterior-most part of the prefrontal cortex (PFC). This cortical region generally overlaps with Brodmann's Area (BA) 10 as defined by cytoarchitectonic methods. FP is considerably larger in the human brain as compared to the ape brain, although the frontal lobe in the humans and great apes occupy a similar proportion of the cerebral cortex (Semendeferi et al. 2001). Additionally, BA 10 is probably the single largest cytoarchitectonic area of the human PFC (Ramnani and Owen 2004). This area is distinguishable from the rest of the PFC in its cytoarchitectonic structure (Ongur et al. 2003) and has a remarkably homogeneous appearance, without exaggeration in the appearance of any of the six cortical layers (Semendeferi et al. 2001). BA 10 is suggested to have undergone a selective reorganization and shift to the more rostral prefrontal region in the hominoid brains, from its restricted location in the orbitofrontal region in the more ancestral

primates (Semendeferi et al. 2001). Being possibly the last brain region to achieve myelination (Burgess et al. 2006), it is likely that the FP has a critical role to play in complex aspects of human cognition, since areas that achieve myelination the latest are thought to be involved in the most complex of functions that are related to the organism's experience (Fuster 1997).

The majority of studies on the FP have focused on functional aspects of this important brain area using functional imaging techniques (reviews, Burgess et al. 2006; Gilbert et al. 2006). Reviewing previous fMRI and PET studies of the PFC, with specific reference to the FP, the above authors concluded that local haemodynamic changes occur in BA 10 during the performance of a wide variety of cognitive tasks. However, FP activation was not sensitive to the precise nature of the stimuli, the precise nature of the intended action or the response method, nor was it related to task difficulty. This led the authors to propose that the FP acts as a "gateway" that biases the priority of information from stimulus-oriented and stimulus-independent thought streams. BA 10 has also been posited to be a crucial node of the "executive attention network", which is involved in conflict resolution, where different neural networks compete for control of consciousness or output (Posner et al. 2006).

There have been relatively few studies of the FP in populations of subjects with neuropsychiatric disorders, despite the relevance of the structure for disorders in which there are disturbances of executive function. However, Vogeley et al. (2003) demonstrated significant reductions of the gray-level index (GLI) in BA 10 in post-mortem brains of schizophrenia subjects. In vivo volumetric studies of the FP in such populations are limited by the lack of a well-accepted definition of the posterior extent of the FP; i.e., the absence of a clear sulcal demarcation of BA 10. Previous in vivo volumetric studies of the FP in schizophrenia have utilized variable definitions of the FP; e.g., the anterior-most 25 slices (25 × 1 mm = 2.5 cm) (Tisserand et al. 2002); the anterior-most 10 slices (10 × 1.5 mm = 1.5 cm) (Wible et al. 1997); upto the termination of the anterior horizontal ramus of the Sylvian fissure (Goldstein et al. 1999; Kennedy et al. 1998; Rademacher et al. 1992). While easy to implement, these landmarks were not chosen on the basis of their putative validity as a posterior boundary of BA 10, the cytoarchitectonic equivalent of the FP.

As mentioned above, there is no natural sulcal boundary to delimit the FP (BA10) on MR images from the adjacent prefrontal cortical subdivisions; i.e., the superior, middle and inferior frontal gyri on the lateral convexity, the medial aspect of the SFG, the rostro-medial prefrontal cortex and the gyrus rectus on the sagittal aspect, and the orbital gyri and inferior aspect of the gyrus rectus on the orbital surface (John et al. 2006).

In a recent MRI-based parcellation study of the prefrontal gyri, based on a careful examination of the cytoarchitectonic maps of Brodmann (1909), Sarkisov (1955) and Economo and Koskinas (1925), as well as by reviewing the observations made by Ongur et al. (2003) (Fig. 1), Semendeferi at al. (2001) and Hof et al. (1995), we proposed the coronal plane containing the anterior termination of the olfactory sulcus (ATOS), as a landmark for demarcating the posterior boundary of the FP (John et al. 2006). The cytoarchitectonic basis for choosing this landmark was detailed in the above-mentioned paper.

In the present study, we describe a reliable method for in vivo volumetric estimations of the FP in healthy subjects using the above landmark. Parcellation of the FP was carried out by manual segmentation, employing this landmark-based definition of its posterior boundary, which, in our opinion, best demarcates the cytoarchitectonically homogeneous FP (BA 10) from more posterior prefrontal subdivisions.

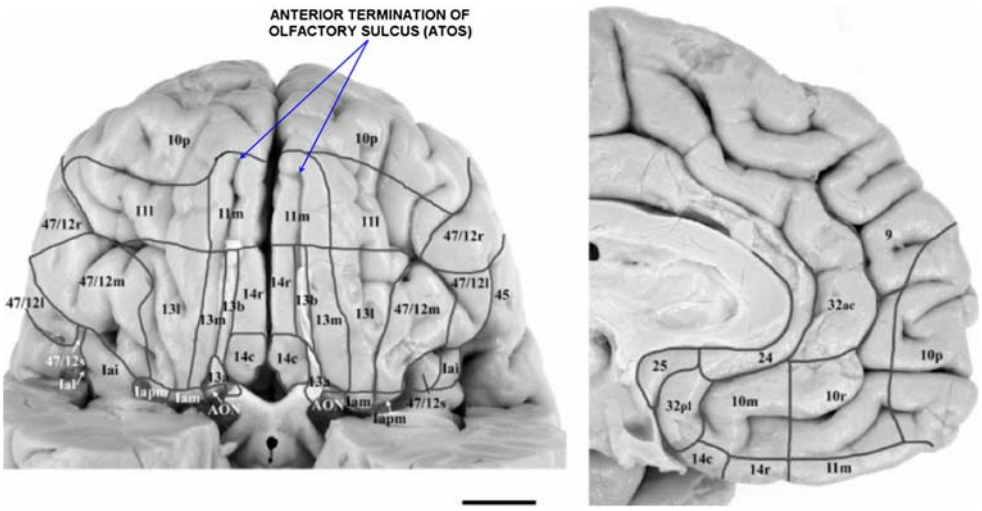

Fig. 1 Cytoarchitectonic subdivisions of the human orbital and medial surfaces (Dost Ongur et al. 2003, © Wiley-Liss, Inc., 2003, reprinted with permission of Wiley-Liss, Inc., a subsidiary of John Wiley & Sons, Inc.), depicting the relation between the posterior boundary of BA 10 and the anterior termination of the olfactory sulcus

Materials and methods

The study was carried out at the National Institute of Mental Health and Neurosciences (NIMHANS), Bangalore, India, with due approval from the NIMHANS Ethical Committee, thus conforming to the ethical standards laid down in the 1964 Declaration of Helskinki. Written informed consent was obtained from all the subjects after complete description of the study.

Subjects

MR scans of 20 normal healthy volunteers (male:female = 7:13) with a mean age of 31.15 years (SD = 5.26, range 22–40) were acquired. These healthy volunteers were ascertained to have no present or past neuropsychiatric disorders, head injury with loss of consciousness or any history of neurological illness and substance abuse or dependence. Axis I and II psychiatric disorders were ruled out by a trained research assistant using the mini international neuropsychiatric interview (MINI)-Plus (Sheehan et al. 1998). In addition, psychotic disorders in the first-degree relatives of these healthy subjects were ruled out using an unstructured clinical interview.

Image acquisition and pre-processing

MR scans were acquired on a Siemens MAGNETOM Vision 1.5 Tesla MRI machine at NIMHANS using an MPRAGE sequence (TR = 9.7 ms, TE = 4 ms, flip angle = 10°, section thickness = 1.25 mm, field of view = 256 × 256 mm, matrix = 256 × 256, number of acquisitions = 3, number of slices = 128, orientation = sagittal, scanning time = 6 min 36 s) that acquires 1.25 × 1 × 1 mm voxels across the entire cranium.

The raw MR data were reformatted using Analyze™ 7.0 software (Robb et al. 1989) from signed 16 bit to unsigned 8 bit MR data sets, using the voxel intensities in the corpus callosum (CC) and the lateral ventricles as limiting values. MR scans were then reoriented to transverse plane and interpolated in to 0.5 × 0.5 × 0.5 mm isotropic voxels using trilinear interpolation. The scans were then rotated in to AC–PC coordinates using Mayo 3D brain Atlas module of Analyze™ 7.0 software.

Manual segmentation and parcellation methods

The segmentation guidelines for parcellation of the FP were as described in John et al. (2006). Briefly, the coronal plane perpendicular to the AC–PC plane and passing through the ATOS was identified and taken as the posterior limit of the FP (Fig. 2), which was then manually outlined on the successive coronal slices anterior to this section till the most rostral section containing gray matter (Fig. 3). Two raters (Y.B.S. and V.R.) were trained in the application of this landmark-based parcellation of FP using a "learning set" of three MR scans. The raters were trained to correctly identify the ATOS considering the normative olfactory sulcal anatomical patterns as described in Duvernoy et al. (1999) and Ono et al (1990). The trained raters then performed independent manual segmentation on a "test set" of five MR scans (both hemispheres) selected from a pool of available MR scans of normal subjects. The inter-rater reliability of FP gray matter volumes generated by the two raters was estimated by calculating the standardized item alpha. Further, the inter-rater reliability of estimating the slice containing the ATOS in the "study set" of 20 MRIs, as represented by the number of coronal slices comprising the FP, was additionally estimated by calculating the standardized item alpha between two raters (Y.B.S. and V.R.).

After establishment of inter-rater reliability, the 20 MR scans were segmented by one of the trained raters (Y.B.S.) by manually outlining the contour of the gray matter of FP in both hemispheres on successive coronal slices (Fig. 3) using Analyze™ 7.0 software (Robb et al. 1989). Total brain volume (TBV), intracranial volume (ICV) and total gray matter volume (TGV) were estimated using the VBM2 module of SPM (http://www.fil.ion.ucl.ac.uk/spm/). Reliability of TBV and TGV estimates using SPM2 and

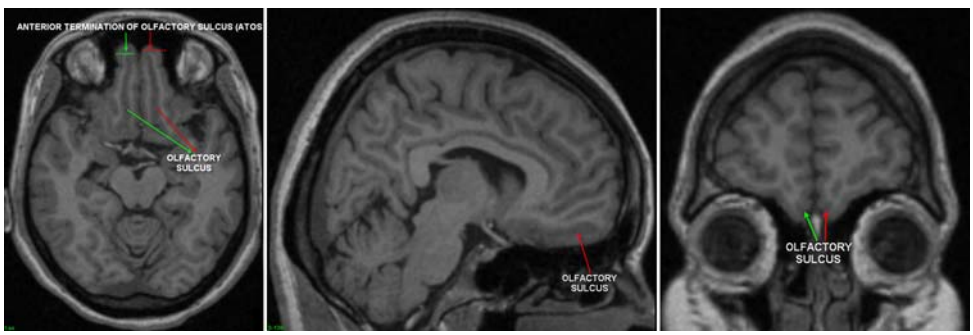

Fig. 2 Identification of the anterior termination of the olfactory sulcus (ATOS) on MR images

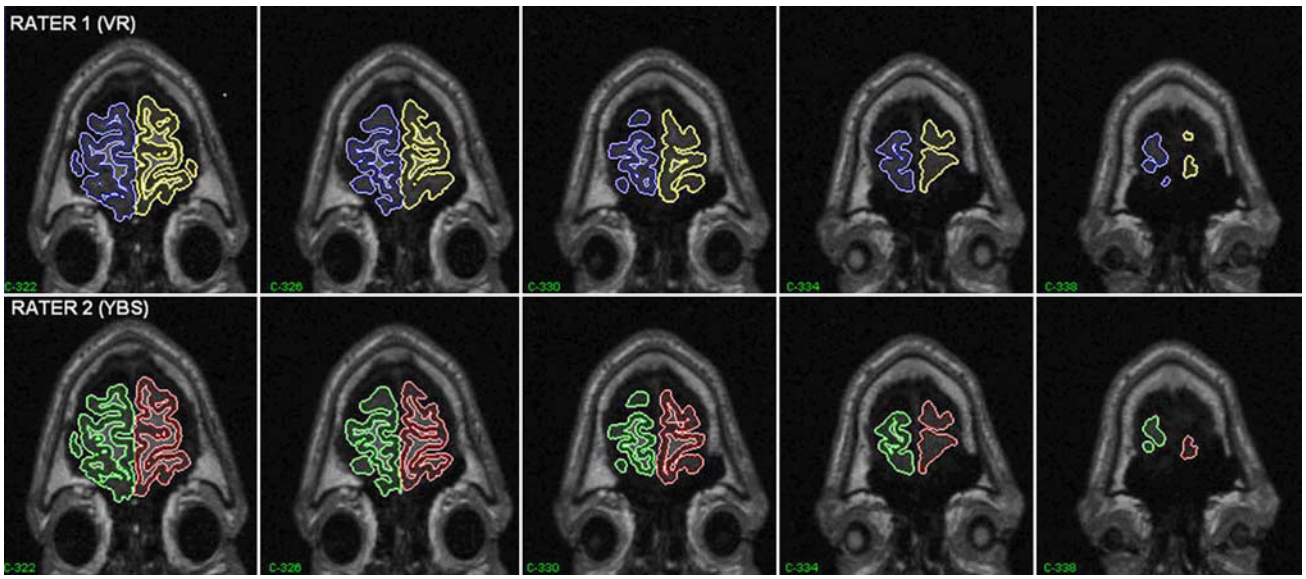

Fig. 3 Manual outlining of the frontal pole (FP) gray matter on successive coronal slices by two raters

Analyze™-based manual segmentation methods was estimated on three test brains (standardized item alpha = 0.99). Volumetric measures of the parcellated FP gray matter were generated using Analyze™ 7.0. The FP gray matter volumes relative to TBV and TGV were also computed.

Statistical analysis

Descriptive statistics were expressed as mean and standard error (SE) of the FP gray matter volumes, ICV, TBV and TGV. Normal distribution of the volumetric measures was assessed using Shapiro–Wilks test of normality. Since all the volumetric measures were normally distributed, parametric statistics were used for subgroup comparisons. Correlation between age and educational status with FP gray matter volumes was carried out using Pearson's product moment correlation. Right vs. left hemisphere comparison of FP gray matter volumes was made using general linear model (GLM) repeated measures analysis of co-variance (RMANCOVA), with TBV and ICV as co-variates. Gender-wise comparisons of FP gray matter volumes were carried out using GLM analysis of covariance (ANCOVA), with TBV as co-variate.

Results

Inter-rater reliability

Inter-rater reliability of estimation of FP volumes (10 volumetric measurements: left = 5, right = 5) using manual segmentation method on five MRI scans by two independent raters was 0.92. Inter-rater reliability of identification of the slice containing the ATOS on the study set of 20 MRIs was 0.99 and 0.97 for the right and left hemispheres, respectively.

Volumetric measurements

Application of our landmark-based definition for parcellation of the FP on MR scans of 20 healthy subjects yielded a mean right FP gray matter volume of 8.421 cm^3 (SE = 0.773, range 3.107–15.741), mean left FP gray matter volume of 8.039 cm^3 (SE = 0.708, range 2.234–12.956) and mean total FP gray matter volume of 16.460 cm^3 (SE = 1.371, range 5.341–27.319). Age and educational status (measured as the number of years of formal education) of the subjects showed no significant correlation with the volumetric measures. There was no significant right–left asymmetry of FP gray matter volume estimates ($F = 1.541$, $P < 0.231$).

The mean number of slices (thickness 0.5 mm) included as FP in right hemisphere was 26.2 (range 18–40), yielding a mean rostro-caudal span of 13.1 mm, whereas on the left hemisphere, a mean of 26.35 slices were included (range 16–34) yielding a mean rostro-caudal span of 13.2 mm.

The mean FP gray matter volume and SE (cm^3) in male and female healthy subjects is given in Table 1. There were no significant gender-wise differences in the right, left and total FP volumes. Males had significantly larger ICV as compared to females on GLM univariate ANOVA ($F = 12.873$, $P < 0.002$). Further, males had significantly greater TBV when compared to females ($F = 8.223$, $P < 0.01$) on GLM ANOVA; however, when ICV was

Table 1 Gender wise comparison of frontal pole volumetric estimates, intracranial volumes, total brain volumes and total gray matter volumes

Volume (cm^3)	Male (n = 7) mean (SE)	Female (n = 13) mean (SE)	F	P
Frontal pole-gray matter				
Right	9.336 (0.840)	7.928 (1.099)	0.229	0.638, NS
Left	9.596 (0.603)	7.201 (0.978)	0.631	0.438, NS
Total	18.932 (1.022)	15.129 (1.969)	0.455	0.509, NS
Intra cranial volume (ICV)	1365.673 (52.427)	1182.524 (25.059)	12.873	0.002
Total brain volume (TBV)	1039.498 (39.650)	925.968 (19.991)	8.223	0.010
Total gray volume (TGV)	652.636 (22.629)	585.572 (12.535)	8.004	0.011

used as a covariate in a GLM univariate ANCOVA, the above significant difference disappeared and in fact, females showed a trend towards increased total brain volume ($F = 3.419$, $P < 0.082$). Males had significantly greater absolute TGV as compared to females ($F = 8.004$, $P < 0.011$), on ANOVA; however, when TBV was used as a covariate in the GLM ANCOVA, this significant difference disappeared ($F = 0.016$, $P < 0.902$).

The right FP gray matter constituted a mean of 0.87% (SE = 0.08, range 0.32–1.71) of the TBV and 1.38% (SE = 0.12, range 0.51–2.72) of the TGV. The left FP gray matter volume constituted a mean of 0.83% (SE = 0.07, range 0.23–1.36) of the TBV and 1.31% (SE = 0.11, range 0.37–2.21) of the TGV. Further, the total FP gray matter constituted 1.70% (SE = 0.14, range 0.54–2.91) of the TBV and 2.69% (SE = 0.22, range 0.88–4.64) of the TGV.

Discussion

The present study describes the use of a reliable, MRI-based method for parcellation of the FP utilizing a landmark for defining the posterior boundary of the FP derived from the cytoarchitectonic literature. The findings in this paper confirm and extend those of prior parcellation studies of the rostral PFC (John et al. 2006; Ongur et al. 2003; Semendeferi et al. 2001; Wible et al. 1997).

The cytoarchitectonic basis for choosing the coronal plane containing the ATOS as the posterior limit of the FP is detailed in John et al. (2006). Briefly, the ATOS was chosen as a reference guide to separate the FP from the rest of the frontal lobe inferiorly and medially, based on the fact that it appears to separate BA 10 in front from BA 11 behind on the orbital surface and area 10r on the medial surface (Ongur et al. 2003) (Fig. 1), in the absence of any naturally occurring sulcal separation between FP and the posterior structures. Interestingly, the same landmark separates the BA 10 from the other chemoarchitectonically defined posterior orbitofrontal zones in the study by Hof et al. (1995) (Fig. 11, pp. 64). The utility of this landmark is further exemplified in a comparative examination of the classical parcellations of the orbitofrontal cortex by Hof et al. (1995) (Fig. 12, p. 65). It is evident from this comparison that the plane of the ATOS closely approximates the posterior extent of BA 10 on the orbitofrontal aspect in the map of Economo and Koskinas (1925). Further, the demarcation between BA 10 from the posterior cytoarchitectonic areas in the maps of Brodmann (1909) (lateral and medial aspects) and Sarkisov (1955) (medial aspect) also closely approximate the location of the coronal plane of the ATOS. However, it must be kept in mind that none of the above classic parcellations or any of the subsequent cyto- or chemo-architectonic studies have specifically addressed the issue of the range of variability between the ATOS and the posterior border of BA 10 in large samples of adult human brains. Nevertheless, in the absence of a clear sulcal demarcation, the evidence discernible from the works of Ongur et al. (2003), Hof et al. (1995) and Semendeferi et al. (2001), when taken together with the congruent evidence from the classical map of Economo and Koskinas (1925), as well as those of Brodmann (1909), and Sarkisov (1955), provide compelling reasons for adopting this landmark-based definition of the posterior boundary of the FP that overlaps with BA 10.

Olfactory sulcus (OS) is the least variable orbitofrontal sulcus (Chiavaras et al. 2001) and is the first orbitofrontal sulcus to appear during development. The OS has a large area (expressed in sulcal probability maps in standardized stereotaxic proportional space) common to over 90% of individuals (Kringelbach and Rolls 2004). Visible at 16 weeks (Chi et al. 1977), the OS is comparable in its ontogeny to the inter-hemispheric and transverse cerebral fissures (at 8 weeks), the Sylvian fissure and collosal sulcus (at 14 weeks), calcarine fissure (at 16 weeks) and central sulcus (at 20 weeks) (Kringelbach and Rolls 2004).

Table 2 shows the patterns of the anterior and posterior ends of the OS observed in our sample of 20 healthy subjects, as per the earlier descriptions by Ono et al. (1990). The OS was found to be remarkably consistent, showing only minimal structural variations and inter-hemispheric asymmetry. The mean lengths of the OS were 41.50 mm (SD = 3.14, range 34.50–48.0 mm) and 41.95

Table 2 Olfactory sulcus patterns in healthy subjects (n = 20)

Patterns of olfactory sulcus	Right (n)	Left (n)
Anterior end		
Straight	9	10
Medial turn	7	8
Extension to the medial surface	2	2
Lateral turn	2	0
Posterior end		
No lateral extension	12	7
Short lateral extension	7	13
Long lateral extension	1	0

(SD = 2.95, range 37.50–46.50 mm), respectively, on the right and left hemispheres. Further, the plane of the ATOS could be identified with a high inter-rater reliability (right hemisphere = 0.99, left hemisphere = 0.97), which supports its use as an easy-to-identify landmark for FP parcellation that largely overlaps with the cytoarchitectonic distinction between BA 10 and the more posterior cytoarchitectonic subdivisions of the PFC. FP volumetric measurements generated using this landmark-based definition yielded an inter-rater reliability of 0.92, which lends further support to its utility.

There was no gender-wise disparity or hemispheric asymmetry in the FP volumetric measures (Table 1). However, as expected, males had significantly larger ICV, TBV as well as TGV when compared to females.

Comparison with previous MRI-based volumetric studies of the FP

A comparison of the FP volumes of the present study with those reported in previous MRI-based volumetric studies (Fig. 4, Table 3), highlights the variability in the volumes depending on the conventions employed for defining the FP. The total FP volumes reported by Rademacher et al. (1992), Kennedy et al. (1998) and Goldstein et al. (1999) (54.68–59.20 cm^3) are substantially higher than our FP volume estimates (16.46 cm^3). As easily discernible from Fig. 4, the above authors have defined the coronal plane passing through the rostral end of the anterior horizontal ramus of Sylvian fissure as the posterior boundary of FP. Use of this definition of the FP would include BAs 9, 11 and 32 on the medial surface, BAs 9, 46 and 47 on the lateral convexity and BA 11 on the inferior surface in the FP, over and above BA 10, and this resulted in the overestimation of the FP volume in these studies. Definition of the FP as the anterior 25 slices (slice thickness = 1.0 mm, rostro-caudal span of FP = 25 mm) by Tisserand et al. (2002) resulted in a similar overestimation of the FP volume. Among all the previous studies, the results of Wible et al. (1997), who defined FP as the anterior 10 slices (slice thickness = 1.5 mm, rostro-caudal span = 15 mm), best approximates our results. Expectedly, the mean rostro-caudal span of the FP observed in our study (13.1 mm) is similar to the observations of Wible et al. (1997). However, the definition of Wible et al. (1997) will not possibly reflect the inter-individual variability in the extent of BA 10 and therefore of the FP volume, since it relies on a "fixed" definition of the FP as the anterior 15 mm of the brain. Thus, the definition of the posterior boundary of FP on MRIs as the coronal plane containing the ATOS would afford greater accuracy of in vivo FP volumetric estimates that reflect inter-individual variability, considering that such a definition has as its basis, the cytoarchitectonic divisions in the area.

Comparison with previous functional imaging studies of BA 10

In the standard "Co-Planar Stereotaxic Atlas of the Human Brain" by Talairach and Tournoux (1988), the BA 10 is predominantly represented as extending from the anterior-most tip of the brain (+69 mm) to +50 mm in the coronal/verticofrontal axis (pp. 62–63), even though narrow strips of BA 10 have been depicted upto +35 mm. Further, the ATOS is represented in the atlas at +49 to +50 mm (pp. 106–107). In an excellent review paper, Grady (1999) analyzed about 90 PET studies showing prefrontal activation, out of which 47 studies that included tests of episodic memory, semantic retrieval and language, motor memory and classical conditioning, working memory and perception showed activation of BA 10. The reported BA activations ranged from +63 to +41 mm in the verticofrontal axis on the Talairach and Tournoux (1988) proportional grid system. However, 43 out of these 47 studies (91.5%) showed activations at ≥ + 46 mm, which closely approximates the representation of the ATOS in the atlas (+49 to +50 mm). These observations further support our proposal that the present landmark-based parcellation of the FP is functionally more relevant than those suggested by previous authors (e.g., Rademacher et al. 1992; Kennedy et al. 1998; Goldstein et al. 1999; Tisserand et al. 2002).

Comparison with the previous cytoarchitectonic study of FP

To the best of our knowledge, the volume of BA 10 has been reported in only one previous study (Semendeferi et al. 2001). In the said paper, the authors reported the

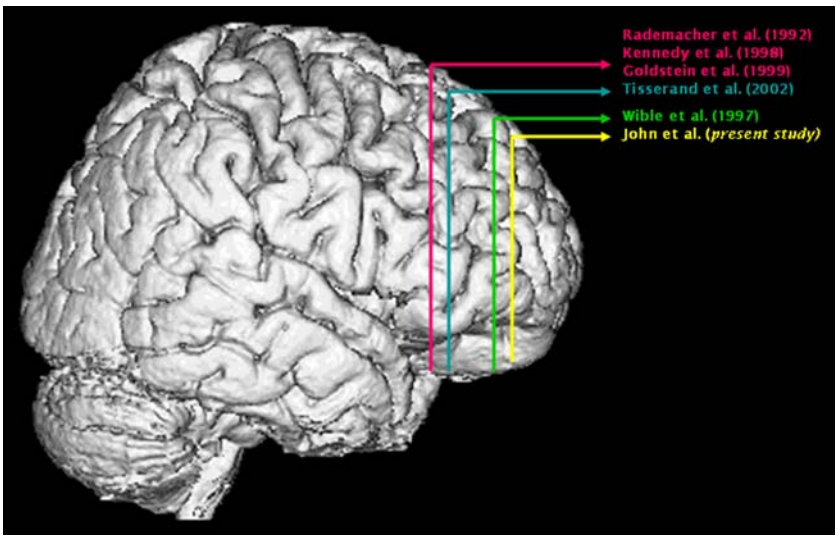

Fig. 4 Comparison of the landmark-based definition of the posterior boundary of the frontal pole in the present study with the landmarks/conventions employed in previous MRI-based volumetric studies

unbiased cortical gray volume estimate of BA 10 of the right hemisphere of a single brain, obtained from histological sections with the use of stereological techniques to be 14.218 cm^3. The estimated right FP gray matter volume in the sample of 20 healthy subjects in the present study ranged from 3.107 to 15.741 cm^3, which encompasses the volume estimate of Semendeferi et al. (2001) obtained from the right hemisphere of a single brain (Fig. 5). Further, their graphic representation of the approximate location of the posterior border of BA 10 of the hominid brain, based on a qualitative cytoarchitectonic evaluation (Semendeferi et al. 2001; Fig. 11, p. 239) closely overlaps with the location of the ATOS plane used in the present study; however, the said diagram, being a schematic representation, precluded any accurate comparisons, and therefore the same cannot be taken as a guide to the exact boundary of the BA 10.

It should be borne in mind that since macroanatomic landmarks and cytoarchitectonical areal boundaries vary independently from each other, the gross anatomical marker proposed in the present paper cannot be taken as a fine level boundary for BA 10. Further, even though the range of FP volumes observed in the present study encompasses the volume estimate of cytoarchitectonically-defined BA 10 in the right hemisphere by Semendeferi et al. (2001), it cannot be presently ruled out that in other brains, the volume of BA 10 may not considerably differ. Therefore, the ATOS landmark for in vivo parcellation of the FP on MR images as proposed in the present paper should still be considered as a "proxy" for the posterior boundary of the BA 10. Cytoarchitectonic examination of the relationship between the ATOS and the posterior border of BA 10 in a large sample of adult human brains would be required for making definitive conclusions regarding the cytoarchitectonic meaningfulness of this landmark. Nevertheless, our results indicate that this could be a better "proxy" landmark for delineating the FP in in vivo MR-based parcellation studies, in view of it being more accurate when compared to existing guidelines for parcellation of the FP in various neuropsychiatric conditions.

In summary, we describe a reliable and potentially valid method for parcellation of the FP, a prefrontal subdivision

Table 3 Comparison of landmarks/conventions followed for definition of the posterior extent of the frontal pole between the present study and previous MRI-based volumetric studies and the estimated total frontal pole volumes

Authors	FP parcellation conventions	Total FP volume (mean ± SD) (cm^3)
Rademacher et al. (1992)	Coronal plane passing through rostral end of the anterior horizontal ramus of Sylvian fissure as the posterior limit of FP	54.68
Kennedy et al. (1998)		59.20 ± 10.5
Goldstein et al. (1999)		56.65 ± 10.36
Tisserand et al. (2002)	Anterior 25 slices (25 × 1.0 mm = 25 mm)	36.76 ± 4.8
Wible et al. (1997)	Anterior 10 slices (10 × 1.5 mm = 15 mm)	17.20
John et al. (present study)	Coronal plane anterior to ATOS as the posterior limit of FP (mean 13.1 mm, range 9–20)	16.46 ± 1.37

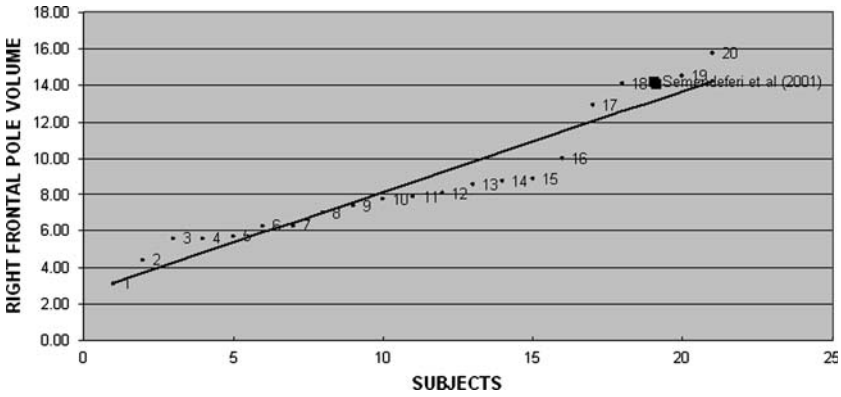

Fig. 5 Graphical representation of the right frontal pole volumes of the individual subjects in the present study (n = 20) in relation to the right hemisphere BA 10 volume reported by Semendeferi et al. (2001)

of central importance in the execution of complex cognitive functions, and therefore, of heuristic importance to a variety of neuropsychiatric conditions. Our results demonstrate how, in the absence of a naturally occurring sulcal boundary, the coronal section containing the ATOS can provide a potentially valid MRI-based landmark for demarcating the FP from the other prefrontal subdivisions. Confirmation of our results by histological examination of the validity of this landmark with the use of stereological techniques would further support its utility in unbiased MRI-based estimation of the FP volumes in various neuropsychiatric conditions. Accurate delineation of the FP afforded by this method will also be an aid in the study of the involvement of this crucial brain region in the performance of various complex cognitive tasks using functional imaging techniques.

Acknowledgments This work was supported by the Fogarty International Research Training in Clinical Sciences fellowship award 5D43TW05811 (J.P.J.). The authors acknowledge the contributions of Dr. Ramesh D. J., M.B.B.S. and Mr. Mohammed Shakeel, M.Phil. (Mental Health and Social Psychology) scholar, in recruiting the subjects for the study as well as establishing inter-rater reliability of the segmentation and parcellation methods.

References

Brodmann K (1909) Vergleichende lokalisationslehre der grosshirnrinde in ihren prinzipien dargestellt auf grund des zellenbaues. Barth, Leipzig

Burgess PW, Simons JS, Dumontheil I, Gilbert SJ (2006) The gateway hypothesis of rostral prefrontal cortex (area 10) function. In: Duncan J, Philips L, Mcleod P (eds) Measuring the mind: speed, control and age. Oxford University Press, Oxford

Chi JG, Dooling EC, Gilles FH (1977) Gyral development of the human brain. Ann Neurol 1:86–93

Chiavaras MM, Legoualher G, Evans A, Petrides M (2001) Three-dimensional probabilistic atlas of the human orbitofrontal sulci in standardized stereotaxic space. Neuroimage 13:479–496

Duvernoy HM (1999) The human brain surface: blood supply and three-dimensional sectional anatomy, 2nd edn. Springer, New York

Economo C, Koskinas GN (1925) Die cytoarchitektonik der hirnrinde des erwachsenen menschen. Wein und. J. Springer, Berlin

Fuster JM (1997) The prefrontal cortex: anatomy, physiology, and neuropsychology of the frontal lobe. Lippincott-Raven, Philadelphia

Gilbert SJ, Spengler S, Simons JS, Steele JD, Lawrie SM, Frith CD, Burgess PW (2006) Functional specialization within rostral prefrontal cortex (area 10): a meta-analysis. J Cogn Neurosci 18:932–948

Goldstein JM, Goodman JM, Seidman LJ, Kennedy DN, Makris N, Lee H, Tourville J, Caviness VS Jr, Faraone SV, Tsuang MT (1999) Cortical abnormalities in schizophrenia identified by structural magnetic resonance imaging. Arch Gen Psychiatry 56:537–547

Grady CL (1999) Neuroimaging and activation of the frontal lobes. In: Miller BL, Cummings JL (eds) The human frontal lobes: functions and disorders. Guilford Series

Hof PR, Mufson EJ, Morrison JH (1995) Human orbitofrontal cortex: cytoarchitecture and quantitative immunohistochemical parcellation. J Comp Neurol 359:48–68

John JP, Wang L, Moffitt AJ, Singh HK, Gado MH, Csernansky JG (2006) Inter-rater reliability of manual segmentation of the superior, inferior and middle frontal gyri. Psychiatry Res 148:151–163

Kennedy DN, Lange N, Makris N, Bates J, Meyer J, Caviness VS Jr (1998) Gyri of the human neocortex: an MRI-based analysis of volume and variance. Cereb Cortex 8:372–384

Kringelbach ML, Rolls ET (2004) The functional neuroanatomy of the human orbitofrontal cortex: evidence from neuroimaging and neuropsychology. Prog Neurobiol 72:341–372

Ongur D, Ferry AT, Price JL (2003) Architectonic subdivision of the human orbital and medial prefrontal cortex. J Comp Neurol 460:425–449

Ono M, Kubik S, Abernathey CD (1990) Atlas of cerebral sulci Georg Thieme Verlag, New York

Posner MI, Sheese BE, Odludas Y, Tang Y (2006) Analyzing and shaping human attentional networks. Neural Netw 19:1422–1429

Rademacher J, Galaburda AM, Kennedy DN, Filipek PA, Caviness JVS (1992) Human cerebral cortex: localization, parcellation, and morphometry with magnetic resonance imaging. J Cogn Neurosci 4:352–374

Ramnani N, Owen AM (2004) Anterior prefrontal cortex: insights into function from anatomy and neuroimaging. Nat Rev Neurosci 5:184–194

Robb RA, Hanson DP, Karwoski RA, Larson AG, Workman EL, Stacy MC (1989) Analyze: a comprehensive, operator-interactive software package for multidimensional medical image display and analysis. Comput Med Imaging Graph 13:433–454

Sarkisov SA (1955) Atlas tsitoarkhitektoniki kory bol'shogo mozga chelovegka. Institut mozga. Akademiia meditsinskikh nauk, SSSR

Semendeferi K, Armstrong E, Schleicher A, Zilles K, Van Hoesen GW (2001) Prefrontal cortex in humans and apes: a comparative study of area 10. Am J Phys Anthropol 114:224–241

Sheehan DV, Lecrubier Y, Sheehan KH, Amorim P, Janavs J, Weiller E, Hergueta T, Baker R, Dunbar GC (1998) The mini-international neuropsychiatric interview (MINI): the development and validation of a structured diagnostic psychiatric interview for DSM-IV and ICD-10. J Clin Psychiatry 59(Suppl 20):22–33, quiz 34–57

Talairach J, Tournoux P (1988) Co-planar stereotaxic atlas of the human brain. Georg Thieme Verlag, New York

Tisserand DJ, Pruessner JC, Sanz Arigita EJ, Van Boxtel MP, Evans AC, Jolles J, Uylings HB (2002) Regional frontal cortical volumes decrease differentially in aging: an MRI study to compare volumetric approaches and voxel-based morphometry. Neuroimage 17:657–669

Vogeley K, Tepest R, Schneider-Axmann T, Hutte H, Zilles K, Honer WG, Falkai P (2003) Automated image analysis of disturbed cytoarchitecture in Brodmann area 10 in schizophrenia. Schizophr Res 62:133–140

Wible CG, Shenton ME, Fischer IA, Allard JE, Kikinis R, Jolesz FA, Iosifescu DV, Mccarley RW (1997) Parcellation of the human prefrontal cortex using MRI. Psychiatry Res 76:29–40